Novel lipid mixtures based on synthetic ceramides reproduce the unique stratum corneum lipid organization

Miranda W. de Jager,* Gert S. Gooris,* Igor P. Dolbnya,[†] Wim Bras,[†] Maria Ponec,[§] and Joke A. Bouwstra[1],*

Leiden/Amsterdam Center for Drug Research,* Department of Drug Delivery Technology, University of Leiden, Leiden, The Netherlands; Netherlands Organization for Scientific Research,[†] Dutch-Belgium Beam-Line Collaborative Research Group, European Synchrotron Radiation Facility, Grenoble, France; and Department of Dermatology,[§] Leiden University Medical Center, Leiden, The Netherlands

Abstract Lipid lamellae present in the outermost layer of the skin protect the body from uncontrolled water loss. In human stratum corneum (SC), two crystalline lamellar phases are present, which contain mostly cholesterol, free fatty acids, and nine types of free ceramides. Previous studies have demonstrated that the SC lipid organization can be mimicked with model mixtures based on isolated SC lipids. However, those studies are hampered by low availability and high interindividual variability of the native tissue. To elucidate the role of each lipid class in the formation of a competent skin barrier, the use of synthetic lipids would offer an alternative. The small- and wide-angle X-ray diffraction results of the present study show for the first time that synthetic lipid mixtures, containing only three synthetic ceramides, reflect to a high extent the SC lipid organization. Both an appropriately chosen preparation method and lipid composition promote the formation of two characteristic lamellar phases with repeat distances similar to those found in native SC. From all synthetic lipid mixtures examined, equimolar mixtures of cholesterol, ceramides, and free fatty acids equilibrated at 80°C resemble to the highest extent the lamellar and lateral SC lipid organization, both at room and increased temperatures.—de Jager, M. W., G. S. Gooris, I. P. Dolbnya, W. Bras, M. Ponec, and J. A. Bouwstra. Novel lipid mixtures based on synthetic ceramides reproduce the unique stratum corneum lipid organization. *J. Lipid Res.* 2004. **45:** 923–932.

Supplementary key words permeability • skin • X-ray diffraction

One of the most important functions of the skin is to serve as a barrier to protect the body against uncontrolled water loss and to prevent the penetration of harmful agents. The protective function of the skin is provided primarily by the stratum corneum (SC), the outermost layer of the skin. SC has a unique morphology, in which keratin-filled corneocytes are surrounded by multilamellar lipid regions (1). The highly ordered intercellular lipid matrix is considered to play a crucial role in the maintenance of the barrier properties of the skin. Therefore, knowledge of the composition and organization of the SC lipids is essential to increase our insight into the skin barrier function.

The composition of the SC lipids differs from that of biological membranes, because phospholipids are nearly absent. Ceramides (CER) belong to the major lipid species in the SC. Together with cholesterol (CHOL) and long-chain free fatty acids (FFA), they form the highly ordered intercellular lipid lamellae. At least nine different free CER types have been identified in human SC (2–5), which are classified as CER1 to CER9. The CER are composed of a sphingosine (S), a phytosphingosine (P), or a 6-hydroxy-sphingosine (H) base to which a nonhydroxy (N) or α-hydroxy (A) fatty acid is chemically linked. The molecular structures of the CER, together with the two nomenclatures, are illustrated in **Fig. 1A**. CER1 (EOS), CER4 (EOH), and CER9 (EOP) have a unique molecular structure in that they contain linoleic acid bound to an ω-hydroxy fatty acid (EO) with a chain length of ~30–32 carbon atoms.

The lipids in the SC are organized in two coexisting crystalline lamellar phases: the short periodicity phase (SPP), with a repeat distance of ~6 nm, and the long periodicity phase (LPP), with a periodicity of ~13 nm (6–8). Both the molecular organization of the LPP and the predominantly crystalline nature of its lipid packing in the presence of substantial amounts of CHOL are unique and are, therefore, suggested to be crucial for the barrier function of the skin.

To elucidate the role of each lipid class in the formation of a competent skin barrier, the phase behavior of the SC lipids has been studied extensively. Using small- and wide-

[1] To whom correspondence should be addressed.
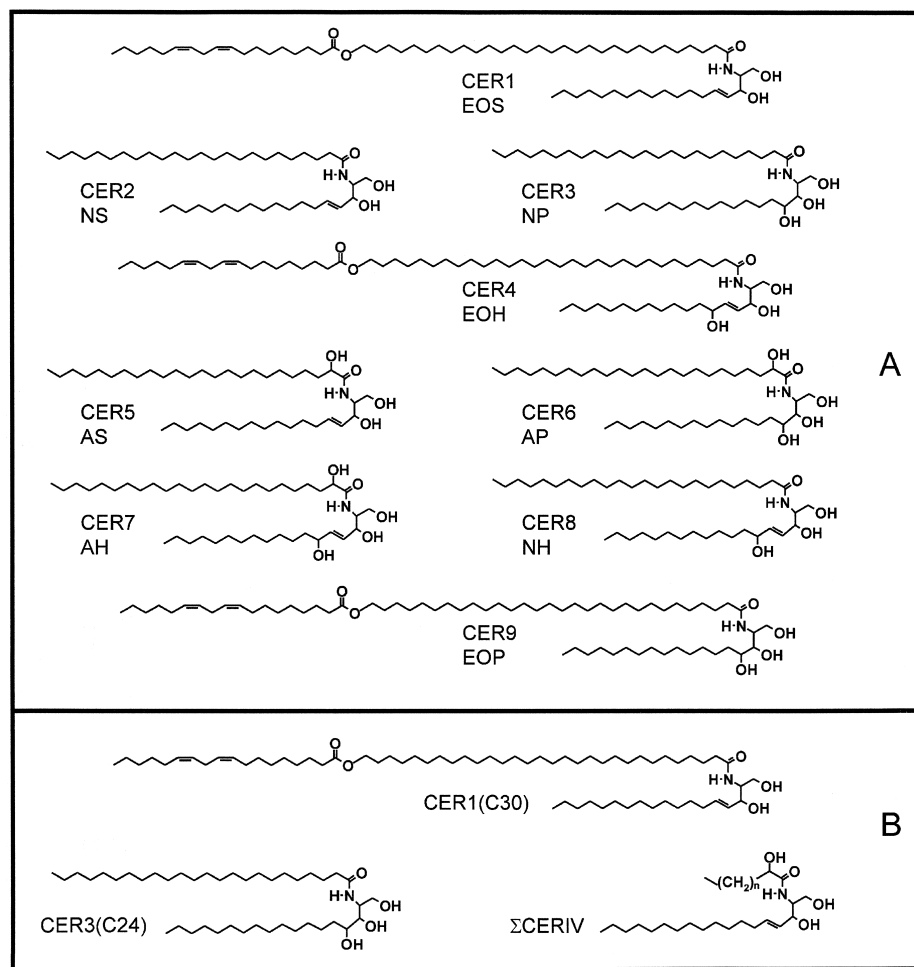   e-mail: bouwstra@chem.leidenuniv.nl

Fig. 1. A: The molecular structures of the ceramides (CER) present in human stratum corneum, indicated according to the numbering system (based on chromatographic migration) and according to their structures. A, α-hydroxy fatty acid; H, 6-hydroxysphingosine; N, nonhydroxy fatty acid; P, phytosphingosine; S, sphingosine. B: The molecular structures of the synthetic CER used in this study. The acyl chain lengths of CER1 (C30) and CER3 (C24) are very well-defined, whereas bovine brain CER type IV (ΣCERIV) shows a distribution in chain lengths, with C18 and C24 as the most abundantly present.

angle X-ray diffraction, it has been demonstrated that mixtures of CHOL, FFA, and CER isolated from either pig or human SC (natCER) closely mimic the lipid organization found in the SC. The results further reveal that in particular, CHOL and CER play a key role in the formation of the LPP, whereas FFA are required to induce the orthorhombic packing of the lipids (9–11).

Extensive studies with lipids isolated from the SC are hampered by the low availability and interindividual variability of the native tissue. In addition, the isolation and separation of the CER from the SC is very labor intensive. Therefore, the use of synthetic CER (synthCER) can offer an attractive alternative. Moreover, each subclass of natCER shows a variation in acyl chain length (2), whereas synthCER have a well-defined acyl chain length. Thus, synthCER also enable us to study in detail the influence of acyl chain length on the SC lipid phase behavior.

In recent years, several studies have been performed with model mixtures based on synthCER. The most fre-

quently studied mixtures contain CHOL and/or palmitic acid (PA) and the commercially available bovine brain CER type III or type IV (12–17). Other studies focused on mixtures prepared, for instance, with synthetic CER2, CER3, or CER5 (18–22). Using a variety of techniques, it has been determined that the packing of the lipids is mainly orthorhombic. However, the results demonstrate that the lipids are not properly mixed in one lattice but coexist in various phases, enriched in one of the components of the lipid mixture. Moreover, small-angle X-ray diffraction studies reveal that the characteristic LPP is not present in mixtures consisting of bovine brain CER type III, CHOL, and PA (23, 24).

In a recent study, we (25) demonstrated that lamellar phases are formed in mixtures prepared with bovine brain CER type III or type IV. However, no LPP could be detected. In mixtures prepared with synthetic CER3 with an acyl chain length of 24 or 16 carbon atoms, several coexisting phases are present, including crystalline V-shaped

CER structures. These V-shaped structures are different from the lipid organization observed in SC and therefore cannot be considered as representative for SC.

In that study, we also studied the effect of synthetic CER1 on the phase behavior of synthetic skin lipid mixtures. From all of the mixtures examined, only one mixture, containing synthetic CER1 and CER3, CHOL, and FFA, showed phase behavior similar to that of SC. However, the repeat distance of the LPP was slightly shorter than that observed in SC. In the absence of CER1, no LPP was formed. This behavior is similar to that observed with mixtures prepared with isolated CER (11, 24, 26).

The objective of the present study is to generate a lipid mixture containing synthCER that closely mimics the natural SC lipid phase behavior. In a previous study performed with natCER, it became evident that a certain degree of fluidity of the lipid mixture is required for the formation of the LPP (11). Because synthCER with uniform chain lengths form highly crystalline phases, it is reasonable to assume that increased lipid mobility and thus a possible enhancement of the formation of the LPP can be achieved by introducing variations in either acyl chain length or head group architecture. Therefore, in the present study, bovine brain CER type IV (referred to as ΣCERIV) was included in the lipid mixture. ΣCERIV consists of a sphingosine base linked to an α-hydroxy fatty acid with varying acyl chain lengths (Fig. 1B), in which C18 and C24 are the most abundantly present (M. W. de Jager, G. S. Gooris, M. Ponec et al., unpublished results). In addition, the preparation method was optimized to increase the degree of fluidity of the lipids to accomplish LPP formation.

The present study shows that both a proper choice of the lipid composition and an optimal equilibration temperature during sample preparation are crucial for the formation of the LPP in mixtures based on synthCER.

MATERIALS AND METHODS

Materials

Palmitic acid, stearic acid, arachidic acid, behenic acid, docosatrienic acid, lignoceric acid, cerotic acid, CHOL, and ΣCERIV were purchased from Sigma-Aldrich Chemie GmbH (Schnelldorf, Germany). N-(30-Linoleoyloxy-triacontanoyl)-sphingosine [synthetic CER1 (C30)-linoleate] was a gift from Beiersdorf AG (Hamburg, Germany). N-Tetracosanoyl-phytosphingosine [synthetic CER3 (C24)] was generously provided by Cosmoferm B.V. (Delft, The Netherlands). Figure 1B shows the CER used in this study. All organic solvents used were of analytical grade and manufactured by Labscan Ltd. (Dublin, Ireland).

Preparation of the lipid mixtures

All samples were prepared with a CER mixture consisting of CER1, CER3, and ΣCERIV at a molar ratio of 1:7:2. The CER mixture was mixed with CHOL in equimolar ratio. For the preparation of the CHOL:CER:FFA mixtures, the fatty acids C16:0, C18:0, C20:0, C22:0, C22:3, C24:0, and C26:0 were mixed at molar ratios of 1.3, 3.3, 6.7, 41.7, 5.4, 36.8, and 4.7%, respectively. This composition is similar to that found in the native SC. Appropriate amounts of individual lipids dissolved in chloroform-methanol (2:1) were combined to yield mixtures of ∼1.5 mg total dry weight at the desired composition with a total lipid concentration of 7 mg/ml. A Camag Linomat IV was used to apply the lipid mixtures onto mica. This was done at a rate of 4.3 μl/min under a continuous nitrogen stream. The samples were equilibrated for 10 min at appropriate temperatures that varied between 60°C and 100°C and subsequently hydrated with an acetate buffer of pH 5.0. Finally, the samples were homogenized by 10 successive freeze-thaw cycles between −20°C and room temperature, during which the samples were stored under gaseous argon.

Small-angle X-ray diffraction

All measurements were performed at the European Synchrotron Radiation Facility (Grenoble, France) using station BM26B (27). The X-ray wavelength and the sample-to-detector distance were 1.24 Å and 1.7 m, respectively. Diffraction data were collected on a two-dimensional multiwire gas-filled area detector. The spatial calibration of this detector was performed using silver behenate. The samples were mounted in a temperature-controlled sample holder with mica windows. Static diffraction patterns of the lipid mixtures were obtained at room temperature for a period of 10 min. The temperature-induced phase changes were investigated by collecting diffraction patterns while increasing the temperature of the sample from 25°C to 95°C at a rate of 2°C/min. Each successive diffraction curve was collected for a period of 1 min. All measurements were performed at least in duplicate.

Small-angle X-ray diffraction (SAXD) provides information about the larger structural units in the sample, namely the repeat distance of a lamellar phase. The scattering intensity I (in arbitrary units) was measured as a function of the scattering vector q (in reciprocal nanometers). The latter is defined as $q = (4\pi\sin\theta)/\lambda$, where θ is the scattering angle and λ is the wavelength. From the positions of a series of equidistant peaks (q_n), the periodicity, or d-spacing, of a lamellar phase was calculated using the equation $q_n = 2n\pi/d$, where n is the order number of the diffraction peak.

Wide-angle X-ray diffraction

Wide-angle X-ray diffraction (WAXD) provides information about the lateral packing of the lipids within the lamellae. WAXD data were collected on a microstrip gas chamber detector with an opening angle of 60° (28). The sample-to-detector distance was 36 cm and the X-ray wavelength was 1.24 Å. The spatial calibration of the detector was performed with a silicon/CHOL mixture.

The SAXD and WAXD data were collected simultaneously.

RESULTS

Effect of the equilibration temperature during sample preparation

Mixtures consisting of CHOL:[CER1:CER3:ΣCERIV] at a molar ratio of 1:[0.1:0.7:0.2] were equilibrated at different temperatures ranging from 60°C to 100°C. The effect of the equilibration temperature on the lipid phase behavior is summarized in **Table 1**. The corresponding diffraction patterns are described below.

Figure 2A shows the diffraction pattern of a lipid mixture equilibrated at 100°C. A lamellar structure with a repeat distance of 12.2 nm (LPP) is indicated by the presence of six diffraction peaks (q = 0.52, 1.03, 1.54, 2.06,

TABLE 1. The effect of equilibration temperature on the formation of the phases in equimolar cholesterol:synthCER (CHOL:synthCER) mixtures

Temperature	LPP	SPP	CER3		CHOL
°C			nm		
60	—	5.7 (1, 2)	3.7 (1, 2)	—	3.35 (1, 2)
70	12.8 (2)	5.7 (1)	3.7 (1, 2)	—	3.35 (1, 2)
80	12.5 (1, 2, 3)^a	5.7 (1)	3.7 (1, 2)	4.3 (1)	3.35 (1, 2)
90	12.6 (1, 2, 3*)	5.5 (1*, 3*)	3.7 (1, 2)	4.3 (1, 2)	3.35 (1, 2)
95	12.3 (1, 2, 3*, 4, 7)	5.3 (1, 2)	3.7 (1, 2)	4.3 (1, 2)	3.35 (1, 2)
100	12.2 (1, 2, 3*, 4, 6, 7)	5.3 (1, 3)	—	4.3 (1, 2)	3.35 (1, 2)

CER, ceramide; LPP, long periodicity phase; SPP, short periodicity phase; synthCER, synthetic ceramides. * The peak is present as a shoulder. ^{a} 12.5 (1, 2, 3) means that the periodicity of the phase is 12.5 nm and interpretation is based on the first-, second-, and third-order reflections.

3.08, and 3.58 nm^{-1}). The reflections at 1.17 and 3.51 nm^{-1} correspond to the first- and third-order maxima of a lamellar phase with a periodicity of 5.3 nm (SPP). The two sharp peaks at 1.46 and 2.91 nm^{-1} indicate the presence of a 4.3 nm phase, ascribed to crystalline CER3 in a V-shaped morphology (19, 22, 25). The presence of crystalline CHOL in separate domains can be deduced from the reflections at 1.87 and 3.74 nm^{-1}.

A reduction in equilibration temperature from 100°C to 95°C does not affect the formation of the LPP and SPP (data not shown). However, X-ray diffraction patterns of lipid mixtures equilibrated at 95°C reveal the presence of a new structure with a repeat distance of 3.7 nm, as suggested by two reflections at 1.69 and 3.40 nm^{-1}. This phase can be assigned to another crystalline V-shaped structure of CER3 (19, 22, 25). The intensities of the peaks attributed to the 4.3 nm phase are slightly reduced compared with those observed in the samples that were equilibrated at 100°C.

The repeat distance of the LPP increases to 12.6 nm when an equilibration temperature of 90°C is used during sample preparation (Fig. 2A). However, only three reflections can be observed that are attributed to this phase. The periodicity of the SPP has increased slightly to 5.5 nm, as deduced from the first- and third-order reflections. Both reflections show partial overlap with other peaks in the diffraction pattern. Crystalline CHOL and the two coexisting crystalline CER3 phases are also present in the lipid mixture.

The diffraction pattern of the lipid mixture prepared using an equilibration temperature of 80°C is illustrated in Fig. 2B. It is evident that decreasing the equilibration temperature reduces the intensities of the three equidistant reflections attributed to the LPP compared with the intensities of the peaks attributed to the SPP (and to crystalline CER3 and CHOL). The repeat distance of the SPP has changed slightly to 5.7 nm. Additionally, crystalline CHOL and crystalline CER3 are present in the lipid mix-
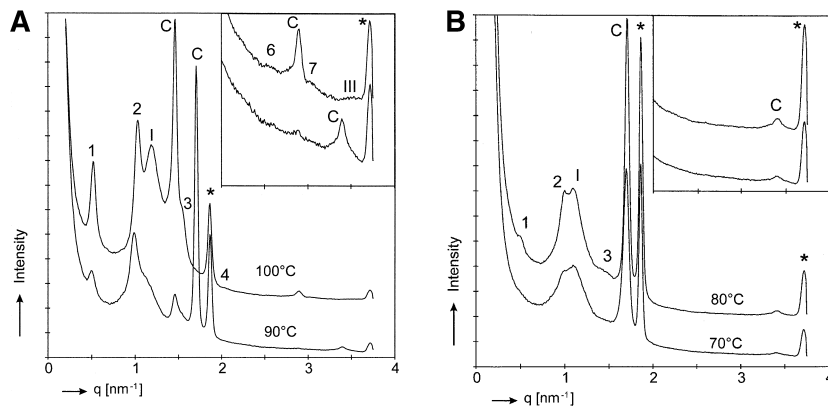

Fig. 2. The effect of equilibration temperature on the phase behavior of equimolar cholesterol:synthetic ceramides (CHOL:synthCER) mixtures. The inset shows a magnification of the reflections in the q range between 2 and 4 nm^{-1}. The Arabic numbers indicate the diffraction orders of the long periodicity phase (LPP), whereas the Roman numbers indicate the diffraction orders of the short periodicity phase (SPP). The letter C refers to the two crystalline phases of CER3. The asterisks indicate the reflections of crystalline CHOL located at 1.87 and 3.74 nm^{-1}. A: Diffraction patterns of mixtures equilibrated at 100°C and 90°C. The various orders of the LPP are located at q = 0.52 nm^{-1} (1), 1.03 nm^{-1} (2), 1.54 nm^{-1} (3), 2.06 nm^{-1} (4), 3.08 nm^{-1} (6), and 3.58 nm^{-1} (7). The various orders of the SPP are located at q = 1.17 nm^{-1} (I) and 3.51 nm^{-1} (III). The reflections at 1.46 and 2.91 nm^{-1} are attributed to crystalline CER3 (4.3 nm phase). B: Diffraction patterns of mixtures equilibrated at 80°C and 70°C. The various orders of the LPP are located at q = 0.49 nm^{-1} (1), 0.99 nm^{-1} (2), and 1.48 nm^{-1} (3). The only reflection attributed to the SPP is located at q = 1.09 nm^{-1} (I). The reflection at 1.46 nm^{-1} is attributed to crystalline CER3 (4.3 nm phase), and the reflections at 1.71 and 3.41 nm^{-1} are attributed to crystalline CER3 (3.7 nm phase).

ture. The latter forms predominantly a 3.7 nm phase, although a weak reflection at 1.46 nm^{-1} indicates that a small fraction of CER3 might still be present as a 4.3 nm phase. A further reduction in the equilibration temperature to 70°C (Fig. 2B) results in a diffraction pattern at which the diffraction peaks attributed to the LPP almost disappear. Only a weak reflection at 0.99 nm^{-1} (second order) reveals that a small fraction of lipids might form a LPP with a periodicity of ∼12.8 nm. Compared with the diffraction pattern of the lipid mixture equilibrated at 80°C, no significant shift is observed in the positions of the reflections attributed to the SPP and crystalline CHOL. All phase-separated CER3 is present as a 3.7 nm phase, because the only two additional reflections observed in the diffraction pattern are located at 1.69 and 3.40 nm^{-1}. Equilibration of the lipid mixture at 60°C (data not shown) does not result in the formation of the LPP. Instead, broad reflections (1.13 and 2.26 nm^{-1}) indicate the presence of a SPP with a repeat distance of 5.7 nm. In addition, crystalline CHOL and crystalline CER3 (3.7 nm phase) can be detected.

The effect of the addition of FFA

To investigate the effect of FFA on the formation of the lamellar phases, FFA were added to the above-mentioned CHOL:[CER1:CER3:ΣCERIV] mixture prepared at a molar ratio of 1:[0.1:0.7:0.2]. Based on the results obtained with the CHOL:synthCER mixtures, the initially chosen equilibration temperature was 95°C. However, equilibration of an equimolar CHOL:synthCER:FFA mixture at this temperature did not result in the formation of the LPP but in melting of the lipids (data not shown). Therefore, the equilibration temperature was reduced to 80°C. The effect of FFA on the phase behavior was examined with CHOL:synthCER:FFA mixtures in which the amount of FFA gradually increased to achieve molar ratios ranging from 1:1:0 to 1:1:1.8. The results are summarized in **Table 2**. The corresponding diffraction patterns are described below. First, the diffraction curve of the CHOL:synthCER:FFA mixture at a molar ratio of 1:1:1 is described (**Fig. 3A**). Subsequently, the effect of decreased and increased FFA content on the lipid phase behavior is presented. The equimolar CHOL:synthCER:FFA mixture shows the presence of a LPP with a repeat distance of 12.2 nm, of which the first five reflections can be detected. The SPP with a periodicity of 5.5 nm is characterized by the

presence of the first three diffraction peaks. Crystalline CHOL and the two coexisting crystalline phases of CER3 with periodicities of 3.7 and 4.3 nm can also be detected in the lipid mixture.

The diffraction pattern of the 1:1:0.75 CHOL:synthCER:FFA mixture is depicted in Fig. 3A. Compared with the equimolar lipid mixture, a slight decrease in the intensities of the reflections attributed to the LPP compared with the intensities of the peaks attributed to the SPP is observed. Furthermore, the peak intensities of the 3.7 nm phase are markedly increased compared with the reflections attributed to the 4.3 nm phase, in contrast to the observations for the equimolar lipid mixture. Additionally, crystalline CHOL can be detected.

A further decrease in FFA content to achieve a molar ratio of 1:1:0.5 results in the diffraction pattern illustrated in Fig. 3B. Compared with the diffraction patterns obtained at higher FFA contents (1:1:0.75 and 1:1:1), the peak intensities of both LPP and SPP are considerably reduced in relation to the peak intensities of the 3.7 nm phase. The first-order reflection of the 3.7 nm phase is now the most prominent peak in the diffraction pattern (q = 1.69 nm^{-1}). Only three orders of the LPP can be detected. Crystalline CHOL is also present in the lipid mixture, and a small fraction of CER3 forms the 4.3 nm phase.

At a CHOL:synthCER:FFA molar ratio of 1:1:0.25 (data not shown), the intensities of the three reflections attributed to the LPP further decreased at the expense of the peak intensities of the 3.7 nm phase. Of the SPP, only the first-order reflection can be detected, which partially overlaps with the second order of the LPP. At this molar ratio, a very small fraction of crystalline CER3 is present as a 4.3 nm phase, because the two reflections attributed to this phase are only weakly present. Crystalline CHOL is again present, derived from the presence of its two reflections.

The diffraction curve of the CHOL:synthCER:FFA mixture at a molar ratio of 1:1:0 is presented in Fig. 3B. Compared with the 1:1:0.25 mixture, the positions and intensities of the diffraction peaks have not changed. A small fraction of lipids forms the LPP and SPP, whereas the peaks of the 3.7 nm phase again dominate the diffraction pattern. Additionally, crystalline CHOL is present in the lipid mixture.

Figure 3C illustrates the effect of increasing the FFA content to levels above equimolar levels. At a molar ratio of 1:1:1.4, four diffraction peaks can be ascribed to the

TABLE 2. The effect of FFA content on the formation of the phases in the lipid mixtures

CHOL:CER:FFA	LPP	SPP	CER3 (C24)		CHOL
			nm		
1:1:0	12.5 (1*, 2, 3)	5.5 (1*)	3.7 (1, 2)	—	3.35 (1, 2)
1:1:0.25	12.5 (1*, 2, 3)	5.5 (1*)	3.7 (1, 2)	—	3.35 (1, 2)
1:1:0.5	12.5 (1, 2, 4)^a	5.5 (1*, 2)	3.7 (1, 2)	4.3 (1, 2)	3.35 (1, 2)
1:1:0.75	12.3 (1, 2, 3*, 4)	5.5 (1, 2, 3)	3.7 (1, 2)	4.3 (1, 2)	3.35 (1, 2)
1:1:1	12.2 (1, 2, 3*, 4, 5)	5.5 (1, 2, 3)	3.7 (1, 2)	4.3 (1, 2)	3.35 (1, 2)
1:1:1.4	12.0 (1, 2, 3*, 4)	5.4 (1, 2)	3.7 (1, 2)	4.3 (1, 2)	3.35 (1, 2)
1:1:1.8	12.0 (1*, 2, 4)	5.6 (1, 2)	3.7 (1, 2)	4.3 (1, 2)	3.35 (1, 2)

* The peak is present as a shoulder.
^{a} 12.5 (1, 2, 4) means that the periodicity of the phase is 12.5 nm and interpretation is based on the first-, second-, and fourth-order reflections.
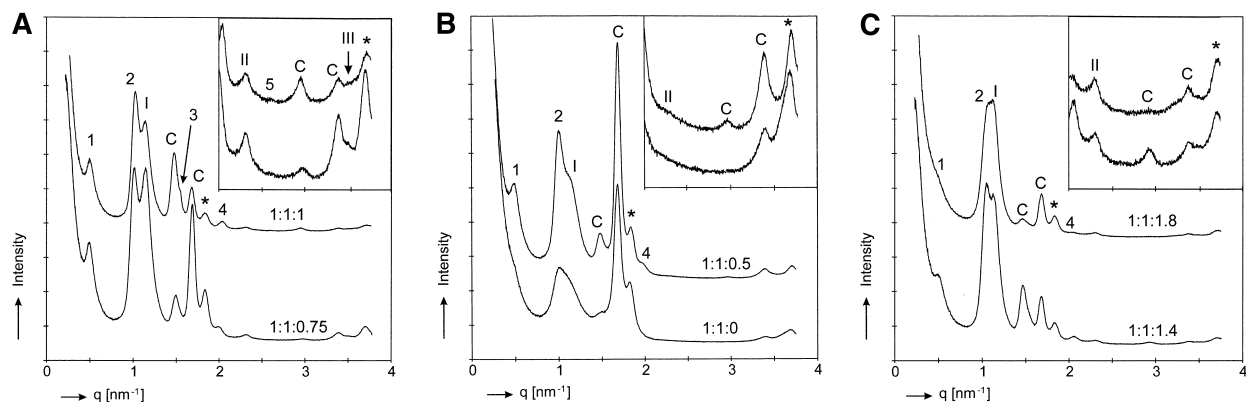
Fig. 3. The effect of FFA content on the phase behavior of CHOL:synthCER:FFA mixtures. The inset shows a magnification of the reflections in the q range between 2 and 4 nm^{-1}. The Arabic numbers indicate the diffraction orders of the LPP, whereas the Roman numbers indicate the diffraction orders of the SPP. The letter C refers to the two crystalline phases of CER3. The asterisks indicate the reflections of crystalline CHOL located at 1.87 and 3.74 nm^{-1}. The reflections at 1.46 and 2.91 nm^{-1} are attributed to crystalline CER3 (4.3 nm phase), and the reflections at 1.71 and 3.41 nm^{-1} are attributed to crystalline CER3 (3.7 nm phase). A: Diffraction patterns of mixtures at a molar ratio of 1:1:1 and 1:1:0.75. The various orders of the LPP are located at q = 0.51 nm^{-1} (1), 1.02 nm^{-1} (2), 1.53 nm^{-1} (3), 2.04 nm^{-1} (4), and 2.56 nm^{-1} (5). The various orders of the SPP are located at q = 1.14 nm^{-1} (I), 2.31 nm^{-1} (II), and 3.47 nm^{-1} (III). B: Diffraction patterns of mixtures at a molar ratio of 1:1:0.5 and 1:1:0. The various orders of the LPP are located at q = 0.50 nm^{-1} (1), 1.00 nm^{-1} (2), and 2.00 nm^{-1} (4). The various orders of the SPP are located at q = 1.12 nm^{-1} (I) and 2.23 nm^{-1} (II). C: Diffraction patterns of mixtures at a molar ratio of 1:1:1.4 and 1:1:1.8. The various orders of the LPP are located at q = 0.52 nm^{-1} (1), 1.05 nm^{-1} (2), and 2.07 nm^{-1} (4). The various orders of the SPP are located at q = 1.12 nm^{-1} (I) and 2.24 nm^{-1} (II).

LLP with a periodicity of 12.0 nm. Furthermore, the SPP (repeat distance of 5.3 nm) is present in the lipid mixture. Compared with Fig. 3A, in which the diffraction pattern of the equimolar lipid mixture is plotted, a slight decrease is observed in the intensities of the reflections attributed to the LPP compared with those attributed to the SPP, as observed for the 1:1:0.75 mixture. The 3.7 and 4.3 nm phases attributed to crystalline CER3 are present, although the peak intensities of the 4.3 nm phase are markedly decreased compared with the equimolar mixture. Additionally, crystalline CHOL can be detected.

The diffraction pattern of the 1:1:1.8 mixture is plotted in Fig. 3C. A very broad peak is observed at 1.12 nm^{-1}, caused by an overlap of the second-order reflection of the LPP and the first-order peak of the SPP. A further reduction is observed in the intensities of the peaks attributed to the LPP compared with those of the SPP. A weak reflection at 1.46 nm^{-1} reveals that only a very small amount of CER3 phase separates into a 4.3 nm phase. Furthermore, crystalline CHOL and the 3.7 nm phase are present in the lipid mixture.

The phase transitions as a function of temperature

The lipid phase behavior of the equimolar CHOL: synthCER and CHOL:synthCER:FFA mixtures (equilibrated at 95°C and 80°C, respectively) has been examined in the temperature range from 25°C to 95°C. In **Fig. 4A, B**, sequential diffraction curves as a function of temperature are presented. Each curve represents the lipid organization during a temperature shift of 2°C. The diffraction pattern of the equimolar CHOL:synthCER mixture at 25°C (Fig. 4A) reveals a number of diffraction peaks that can be assigned to the presence of a LPP and a SPP with

periodicities of 12.6 and 5.4 nm, respectively, similar to that described for Fig. 2A. The reflections attributed to the SPP disappear at ~43°C. In the same temperature region, the reflections (first and second order) of the LPP start to decrease in intensity and disappear at 55°C. Striking is the appearance of a new phase, with a repeat distance of ~9.9 nm, between 59°C and 73°C. This phase might be formed by CER1 that crystallizes in separate domains. In the same temperature region, the reflections of the 3.7 and 4.3 nm phases, both attributed to crystalline CER3, shift slightly to lower q values, corresponding to spacings of 4.0 and 4.5 nm, respectively. The intensities of the peaks attributed to the latter phase markedly increase with increasing temperature, whereas the intensity of the former hardly increases. Both phases are still present at 95°C. The CHOL reflections disappear at a temperature of ~57°C.

The equimolar CHOL:synthCER:FFA mixture shows the presence of two lamellar phases with periodicities of 12.0 and 5.4 nm (Fig. 4B). The intensities of the diffraction peaks attributed to the LPP and SPP hardly change between 25°C and 49°C. A further increase in temperature gradually decreases the intensities of the reflections of the SPP, resulting in a disappearance of this phase at ~59°C. The reflections of the LPP start to decrease in intensity at ~59°C and disappear at 65°C. Similarly, as observed for the CHOL:synthCER mixture, the peaks attributed to the 3.7 and 4.3 nm phases formed by CER3 shift to lower q values. However, the shift of the reflections of the 3.7 nm phase is abrupt at 43°C, whereas the reflection of the 4.3 nm phase gradually shifts over a wide temperature range to a spacing of 4.6 nm at 63°C. At ~45°C, a new phase is formed, of which only one reflection can be detected
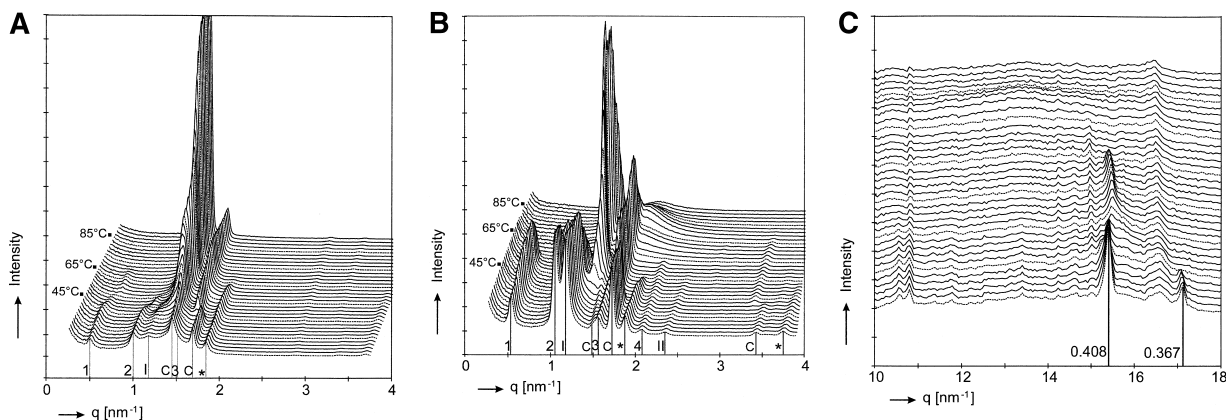
Fig. 4. Changes in lipid phase behavior as a function of temperature. A: The lamellar organization of equimolar CHOL:synthCER mixtures. B: The lamellar organization of equimolar CHOL:synthCER:FFA mixtures. C: The lateral packing of CHOL:synthCER:FFA mixtures. The Arabic numbers indicate the diffraction orders of the LPP, whereas the Roman numbers indicate the diffraction orders of the SPP. The letter C refers to the two crystalline phases of CER3. The asterisks indicate the reflections of crystalline CHOL. The dashed lines represent the diffraction curves at 25, 35, 45, 55, 65, 75, and 85°C.

($q = 1.37 \text{ nm}^{-1}$). The reflection dramatically increases in intensity, being the most prominent peak in the diffraction pattern at increased temperatures. A maximal intensity is reached at ~71°C. A further increase in temperature reduces the peak intensity. The reflections at 1.37 and 1.57 nm^{-1} both disappear between 81°C and 85°C. In this temperature range, a broad peak at 1.90 nm^{-1} is formed, which is still present at 95°C.

Lateral packing of the lipids

A hexagonal lateral packing is characterized by a strong 0.41 nm reflection in the WAXD pattern, whereas the diffraction pattern of an orthorhombic packing is characterized by two strong reflections at 0.41 and 0.37 nm. All lipid mixtures measured during this study are characterized by a large number of strong and weak reflections in the WAXD pattern. In the CHOL:synthCER mixtures, a reflection at 0.41 nm is present, although its intensity is very weak compared with the various strong neighboring reflections attributed to either crystalline CHOL or CER3 (data not shown). Therefore, it cannot be deduced with certainty whether a hexagonal lateral packing is present in the CHOL:synthCER mixtures.

In the equimolar CHOL:synthCER:FFA mixture, two strong 0.408 and 0.367 nm reflections indicate an orthorhombic lateral packing (data not shown). This is already observed at low FFA content, such as in the mixture at a CHOL:CER:FFA molar ratio of 1:1:0.25. A further increase in FFA content in the CHOL:CER:FFA mixture to 1:1:1.8 does not affect the lateral packing but drastically changes the diffraction pattern by weakening the intensities of the numerous CHOL and CER3 reflections. Both SAXD and WAXD data obviously show that an increased FFA content results in reduced intensities of the CHOL and CER3 reflections, indicating an increased solubility of both components in the lamellar phases.

The diffraction patterns of the equimolar CHOL:synthCER:FFA mixture monitored as a function of temperature are plotted in Fig. 4C. The 0.408 and 0.367 nm peaks indicate an orthorhombic lateral packing. Between 35°C and 37°C, the 0.367 nm reflection disappears, indicating an orthorhombic-hexagonal phase transition. The 0.408 nm reflection first decreases in intensity. However, a further increase in temperature increases the intensity of the 0.408 nm reflection slightly, indicating a metastable-to-stable phase change. Similar results were obtained with SC (J. A. Bouwstra and G. S. Gooris, unpublished results). A disappearance of this peak is observed at 65°C, which is the same temperature at which the long periodicity phase disappeared in the SAXD pattern.

DISCUSSION

For detailed studies on the effect of the molecular structure of individual CER on SC lipid organization, the use of synthCER offers an attractive approach, because both the head group and acyl chain composition can be systematically modified. One should be aware, however, that the prerequisite for replacing natCER by synthCER is that their phase behavior reflects that of the SC. The major difference between natCER and synthCER is great variation in acyl chain length in natCER versus well-defined acyl chain length in synthCER. Earlier studies with mixtures prepared with lipids isolated from native SC revealed that the SC phase behavior can be mimicked with simplified CER mixtures, provided that CER1 is present (29). In the present study, a synthCER mixture was used consisting of CER1, CER3, and ΣCERIV mixed in a 1:7:2 ratio, with the relative CER1 content similar to that found in native SC (2). Because a small variation in acyl chain length is expected to reduce lipid mobility, the procedure for the preparation of a homogenous lipid mixture has been adapted and will be discussed below. The results obtained in the present study demonstrate that both the lipid composition

and the temperature at which the samples are equilibrated play important roles in the formation of the LPP.

Influence of equilibration temperature on phase behavior

The formation of the LPP in equimolar CHOL:synthCER mixtures is enhanced when an increased equilibration temperature is used during the sample preparation. The mechanism behind this phenomenon, however, is not yet known, but it will be subject of future studies. It is reasonable to assume that at increased temperatures, the formation of the LPP is promoted up to a certain optimal fluidity or mobility of the hydrocarbon chains. For example, for CHOL:synthCER mixtures equilibrated at 95°C or 100°C, the diffraction patterns are very similar and show a dominant formation of the LPP, indicating that the optimum has most likely been achieved. A further increase to 105°C or 110°C results in melting of the lipids and in decreased formation of the LPP.

Influence of FFA on phase behavior

The addition of FFA to the CHOL:synthCER mixture obviously increases the fluidity of the lipids at increased temperatures, because equilibration at 95°C resulted in melting of the lipids. This is most likely ascribed to the FFA chain length variation from 16 to 26 carbon atoms. It further became evident that for the formation of the LPP, an optimal amount of FFA in CHOL:synthCER:FFA mixtures is required. Systematic increase in FFA content to achieve an equimolar CHOL:synthCER:FFA mixture promotes the formation of the LPP. However, when the relative FFA content further increases, the formation of the LPP is reduced and the SPP dominates. A lower equilibration temperature would probably shift the optimal amount of FFA for the formation of the LPP to higher values, whereas the opposite is true for a higher equilibration temperature. From these observations, we can conclude that for each lipid composition, an optimal equilibration temperature is required.

FFA seem to play an important role in the lipid phase behavior. This conclusion is drawn from the following observations made with CHOL:synthCER:FFA mixtures: *i*) CHOL is better incorporated (dissolved), as reflected by the weaker intensities of the CHOL reflections than seen in the absence of FFA; the same trend is seen with natCER (9, 11); *ii*) the intensities of the peaks attributed to crystalline CER3 are also weaker than those observed in the CHOL:synthCER mixtures, indicating better incorporation of CER3 in the presence of FFA; *iii*) a better ordering of the lamellar structures, because in the presence of FFA, more higher order diffraction peaks can be seen for both LPP and SPP than in the absence of FFA; and *iv*) FFA have a profound effect on lateral packing, because only in their presence is the packing orthorhombic, as observed for lipid mixtures based on isolated pig or human CER (10, 11) and in human SC (30).

Comparison between synthCER and natCER

The potential use of synthCER instead of natCER in studies on SC lipid organization is supported by observations made at increased temperatures. Many similarities can be observed in the lipid phase behavior between CHOL:CER:FFA mixtures containing synthCER and natCER. As far as the lamellar organization is concerned, for mixtures prepared with synthCER, the LPP disappears at ~65°C. This temperature is close to the 63°C found in mixtures prepared with pig natCER (9) and to the 67°C found for mixtures prepared with human natCER (31). With synthCER, the SPP and the reflections of phase-separated CHOL disappear in the same temperature range as observed for mixtures prepared with natCER. Furthermore, in mixtures containing synthCER, a new phase with a repeat distance of 4.6 nm is formed at high temperatures. The formation of a similar phase is observed in lipid mixtures containing natCER, although the periodicity of 4.3 nm differs slightly from that found in the mixtures based on synthCER.

Concerning the changes in lateral packing at increased temperatures, at ~35°C, a phase transition from orthorhombic to hexagonal lateral packing takes place in the CHOL:synthCER:FFA mixture. As described above, no changes in lamellar organization have been noted at this temperature, suggesting that the transition does not affect the lamellar phase behavior. The hexagonal lateral packing disappears at 65°C, which is the same temperature at which the LPP disappears. This suggests that either orthorhombic or hexagonal lateral packing is a requisite for LPP formation. This confirms the findings with natCER, which revealed that when the fraction of lipids in a liquid phase is too high, the formation of the SPP is increased at the expense of the LPP (11).

In spite of many similarities, some differences are observed between mixtures prepared with synthetic and natural lipids. The main difference is the presence of two additional phases with repeat distances of 3.7 and 4.3 nm, respectively, in the mixtures prepared with synthCER. These phases, which are attributed to crystalline CER3, have never been observed in the mixtures containing natCER. From the present study, it is clear that an increase in equilibration temperature from 60°C to 100°C or an increase in FFA content in CHOL:synthCER:FFA mixtures from 1:1:0 to 1:1:1 increases the intensities of the peaks attributed to the 4.3 nm phase at the expense of the 3.7 nm phase. A further increase in the FFA content leads to a

TABLE 3. Relative intensities of the diffraction peaks of the LPP in equimolar CHOL:synthCER:FFA mixtures and equimolar CHOL:pigCER mixtures

Order	12.2 nm Phase CHOL synthCER:FFA	13 nm Phase CHOL pigCER:FFA[a]
1	1.0	1.0
2	2.94 ± 0.36	2.55 ± 0.28
3	0.37 ± 0.06	0.81 ± 0.10
4	0.15 ± 0.02	0.09 ± 0.01
7	0.04 ± 0.03	0.08 ± 0.03

For scaling, the intensity of the first-order diffraction peak of the LPP was set equal to 1. The values are presented as averages (n = 6) ± SD.
[a] M. W. de Jager, G. S. Gooris, M. Ponec et al., unpublished results.

marked reduction of the peak intensities of the 4.3 nm phase. However, under these conditions, the fraction of lipids forming the characteristic LPP is also diminished.

Another difference between the phase behavior of the CHOL:CER:FFA mixtures prepared with synthCER and nat-CER is the repeat distance of the LPP. In the absence of FFA, the periodicity of the LPP in CHOL:synthCER mixtures equilibrated at 95°C or 100°C is ~12.3 nm. The periodicity of the LPP in mixtures prepared with isolated human or pig CER is very similar, 12.8 or 12.2 nm, respectively. The situation is different when FFA are included to reach an equimolar CHOL:natCER:FFA mixture. The repeat distance of the LPP increases slightly to 13.0 and 13.3 nm for human and pig CER, respectively, the same values found in native SC. However, in the CHOL:synthCER:FFA mixture, the repeat distance decreases slightly to ~12.2 nm. In addition to this, we observed that an increase in equilibration temperature or in FFA content led to a slight decrease in the repeat distance of the LPP (Tables 1, 2).

The relative intensities of the various diffraction orders provide information on the relative electron density distribution in the LPP. Therefore, we determined the relative intensities of the various reflections of the LPP in six equimolar CHOL:synthCER:FFA mixtures, measured during four different X-ray diffraction sessions, and compared the values with those obtained with equimolar CHOL:pigCER:FFA mixtures. The results given in **Table 3** indicate that the relative intensities of the peaks attributed to the LPP show the same trend in all samples. However, in the synthCER mixtures, the relative peak intensities of some peaks of the LPP differ from those found in the CHOL:pigCER:FFA mixtures. This indicates that the localization of the lipids within the LPP in mixtures prepared with synthCER might differ slightly.

In conclusion, the results of the present study demonstrate for the first time that one can generate lipid mixtures containing synthetic CER that mimic to a high extent the phase behavior observed in native SC, provided that the experimental conditions are appropriately chosen. Therefore, the composition of the lipid mixtures and the temperature at which the lipid mixtures are equilibrated play crucial roles for the formation of the characteristic LPP. From all of the lipid mixtures tested, the phase behavior of the equimolar CHOL:[CER1: CER3:ΣCERIV]:FFA mixtures resemble to the highest extent the lamellar and lateral SC lipid organization, both at room and increased temperatures.🔒

REFERENCES

1. Elias, P. M. 1983. Epidermal lipids, barrier function, and desquamation. *J. Invest. Dermatol.* **80 (Suppl.):** 44–49.

2. Ponec, M., A. Weerheim, P. Lankhorst, and P. Wertz. 2003. New acylceramide in native and reconstructed epidermis. *J. Invest. Dermatol.* **120:** 581–588.

3. Robson, K. J., M. E. Stewart, S. Michelsen, N. D. Lazo, and D. T. Downing. 1994. 6-Hydroxy-4-sphingenine in human epidermal ceramides. *J. Lipid Res.* **35:** 2060–2068.

4. Stewart, M. E., and D. T. Downing. 1999. A new 6-hydroxy-4-sphingenine-containing ceramide in human skin. *J. Lipid Res.* **4:** 1434–1439.

5. Wertz, P. W., M. C. Miethke, S. A. Long, J. S. Strauss, and D. T. Downing. 1985. The composition of the ceramides from human stratum corneum and from comedones. *J. Invest. Dermatol.* **84:** 410–412.

6. Bouwstra, J. A., G. S. Gooris, J. A. van der Spek, and W. Bras. 1991. The structure of human stratum corneum as determined by small angle X-ray scattering. *J. Invest. Dermatol.* **96:** 1006–1014.

7. Bouwstra, J. A., G. S. Gooris, J. A. van der Spek, and W. Bras. 1991. Structural investigations of human stratum corneum by small angle X-ray scattering. *J. Invest. Dermatol.* **97:** 1005–1012.

8. Bouwstra, J. A., G. S. Gooris, W. Bras, and D. T. Downing. 1995. Lipid organization in pig stratum corneum. *J. Lipid Res.* **36:** 685–695.

9. Bouwstra, J. A., G. S. Gooris, K. Cheng, A. Weerheim, W. Bras, and M. Ponec. 1996. Phase behavior of isolated skin lipids. *J. Lipid Res.* **37:** 999–1011.

10. Bouwstra, J. A., G. S. Gooris, F. E. R. Dubbelaar, A. M. Weerheim, and M. Ponec. 1998. pH, cholesterol sulfate, and fatty acids affect the stratum corneum lipid organization. *J. Invest. Dermatol.* **3:** 69–73.

11. Bouwstra, J. A., G. S. Gooris, F. E. R. Dubbelaar, and M. Ponec. 2002. Phase behavior of stratum corneum lipid mixtures based on human ceramides: the role of natural and synthetic ceramide 1. *J. Invest. Dermatol.* **118:** 606–617.

12. Fenske, D. B., J. L. Thewalt, M. Bloom, and N. Kitson. 1994. Models of stratum corneum intercellular membranes: ^{2}H NMR of microscopically oriented multilayers. *Biophys. J.* **67:** 1562–1573.

13. Kitson, N., J. Thewalt, M. Lafleur, and M. Bloom. 1994. A model membrane approach to the epidermal permeability barrier. *Biochemistry.* **33:** 6707–6715.

14. Moore, D. J., M. E. Rerek, and R. Mendelsohn. 1997. Lipid domains and orthorhombic phases in model stratum corneum: evidence from Fourier transform infrared spectroscopy studies. *Biochem. Biophys. Res. Commun.* **231:** 797–801.

15. Neubert, R., W. Rettig, S. Wartewig, M. Wegener, and A. Wienhold. 1997. Structure of stratum corneum lipids characterized by FT-Raman spectroscopy and DSC. II. Mixtures of ceramides and saturated fatty acids. *Chem. Phys. Lipids.* **89:** 3–14.

16. Percot, A., and M. Lafleur. 2001. Direct observations of domains in model stratum corneum lipid mixtures by Raman microspectroscopy. *Biophys. J.* **81:** 2144–2153.

17. Wegener, M., R. Neubert, W. Rettig, and S. Wartewig. 1997. Structure of stratum corneum lipids characterized by FT-Raman spectroscopy and DSC. III. Mixtures of ceramides and cholesterol. *Chem. Phys. Lipids.* **88:** 73–82.

18. Chen, H., R. Mendelsohn, M. E. Rerek, and D. J. Moore. 2000. Fourier transform infrared spectroscopy and differential scanning calorimetry studies of fatty acid homogeneous ceramide 2. *Biochim. Biophys. Acta.* **1468:** 293–303.

19. Dahlen, B., and I. Pascher. 1979. Molecular arrangements in sphingolipids. Thermotropic phase behaviour of tetracosanoyl-phytosphingosine. *Chem. Phys. Lipids.* **24:** 119–133.

20. Moore, D. J., and M. E. Rerek. 2000. Insights into the molecular organisation of lipids in the skin barrier from infrared spectroscopy studies of stratum corneum lipid models. *Acta Derm. Venereol. Suppl.* **208:** 16–22.

21. Ohta, N., and I. Hatta. 2002. Interaction among molecules in mixtures of ceramide/stearic acid, ceramide/cholesterol and ceramide/stearic acid/cholesterol. *Chem. Phys. Lipids.* **115:** 93–105.

22. Raudenkolb, S., W. Hübner, W. Rettig, S. Wartewig, and R. H. H. Neubert. 2003. Polymorphism of ceramide 3. Part 1. An investigation focused on the head group of N-octadecanoylphytosphingosine. *Chem. Phys. Lipids.* **123:** 9–17.

23. Bouwstra, J. A., J. Thewalt, G. S. Gooris, and N. Kitson. 1997. A model membrane approach to the epidermal permeability barrier: an X-ray diffraction study. *Biochemistry.* **36:** 7717–7725.

24. McIntosh, T. J., M. E. Stewart, and D. T. Downing. 1996. X-ray diffraction analysis of isolated skin lipids: reconstitution of intercellular lipid domains. *Biochemistry.* **35:** 3649–3653.

25. de Jager, M. W., G. S. Gooris, I. P. Dolbnya, W. Bras, M. Ponec, and J. A. Bouwstra. 2003. The phase behaviour of lipid mixtures based on synthetic ceramides. *Chem. Phys. Lipids.* **124:** 123–134.

26. Bouwstra, J. A., G. S. Gooris, F. E. R. Dubbelaar, A. M. Weerheim, A. P. Ijzerman, and M. Ponec. 1998. Role of ceramide 1 in the molecular organization of the stratum corneum lipids. *J. Lipid Res.* **39:** 186–196.

27. Bras, W. 1998. A SAXS/WAXS beamline at the ESRF and future experiments. *J. Macromol. Sci. Phys. B.* **37:** 557–566.

28. Dolbnya, I. P., H. Alberda, F. G. Hartjes, F. Udo, R. E. Bakker, M. Konijnenburg, E. Homan, I. Cerjak, P. Goedtkindt, and W. Bras. 2002. A fast position sensitive MSGC detector at high count rate operation. *Rev. Sci. Instrum.* **73:** 3754–3758.

29. Bouwstra, J. A., G. S. Gooris, F. E. R. Dubbelaar, and M. Ponec. 2000. The lipid organisation in the skin barrier. *Acta Derm. Venereol. Suppl.* **208:** 23–30.

30. Bouwstra, J. A., G. S. Gooris, M. A. Salomons-de Vries, J. A. van der Spek, and W. Bras. 1992. Structure of human stratum corneum as a function of temperature and hydration: a wide-angle X-ray diffraction study. *Int. J. Pharm.* **84:** 205–216.

31. Bouwstra, J. A., G. S. Gooris, F. E. R. Dubbelaar, and M. Ponec. 2001. Phase behavior of lipid mixtures based on human ceramides: coexistence of crystalline and liquid phases. *J. Lipid Res.* **42:** 1759–1770.